Supporting Information

Synergistic chemiluminescence nanoprobe: Au clusters-Cu^{2+}-induced chemiexcitation of cyclic peroxides and resonance energy transfer

Kexin Zhang,[a] Mingxia Sun,[b] Hongjie Song,[a] Yingying Su[b] and Yi Lv[ab]*

a. Key Laboratory of Green Chemistry & Technology, Ministry of Education, College of chemistry, Sichuan university, Chengdu, Sichuan, 610064, China

b. Analytical & Testing Center, Sichuan University, Chengdu 610064, China.

*Corresponding Author. Email: lvy@scu.edu.cn (Lv Y.); Tel & Fax: +86-28-85412798

Materials and methods

1. Chemicals

All chemicals were at least of analytical grade. Bovine serum albumin (BSA, fraction V) was bought from Sigma-Aldrich. $HAuCl_4 \cdot 3H_2O$ was purchased from. Copper chloride was purchased from Chengdu United Institute of Chemical & Reagent. Tetrahydrofuran was purchased from. 2,2,6,6-Tetramethyl-4-piperidie (TEMP), Nitrotetrazolium Blue chloride (NBT), 5,5-Dimethyl-1-pyrroline-N-oxide (DMPO) and 1,3-Diphenylisobenzofuran (DPBF) were purchased from Sigma-Aldrich Chemical Co. (St. Louis, MO, USA). The ultrapure water (18.2 MΩ/cm) used was purified through Mili-Q ultrapure system.

2. Synthesis of four kinds of nanoparticles

All glassware used in the experiment was cleaned in a bath of freshly prepared 3:1 HCl/HNO3 and rinsed in ethanol and ultrapure water three times prior to use.

BSA-Au nanoclusters

The synthetic procedure of Au nanoclusters was outlined based on published literature.[1] Firstly, 25 mL of 10 mM $HAuCl_4$ aqueous solution was added into 25 ml of 50mg/mL BSA solution under vigorous stirring at 37 ℃. After mixed about 2 min, 2.5 mL 1 M NaOH solution was added to adjust pH. Then, the mixture was incubated at 37 ℃ for 12 h. During the reaction time, the color of the mixture changed from light yellow to reddish brown. Finally, the as-synthesized Au NCs (52.5 mL) were dialyzed in dialysis bag with 10000 Da MWCO for 24 h. The final solution was stored at 4 ℃ when not in use.

Tys-Au nanoclusters

The synthetic procedure of Au nanoclusters was outlined based on published literature.[2] All procedures were similar to the above steps, except that the bovine serum protein was replaced with trypsin.

GSH-Au nanoclusters

The synthetic procedure of Au nanoclusters was outlined based on published literature.[3] AuNCs were synthesized

through reduction of HAuCl4 with GSH. Briefly, a fresh 100 × 10^{-3} m GSH aqueous solution (0.15 mL) was added into a 20 × 10^{-3}m $HAuCl_4$ aqueous solution (0.5 mL) and the final mixture was kept in 5 mL under stirring at 70 °C for 24 h.

Citrate-Au nanoparticles

The synthetic procedure of Au nanoclusters was outlined based on published literature.[4] larger than 10-nm-diameter gold nanoparticles were synthesized by the citrate reduction method. A 100-mL sample of aqueous HAuCl4 (0.25 mM) was prepared in a 250-mL flask, containing controlled amounts of HCl or NaOH at room temperature. The solution was brought to boil while being stirred, and the corresponding amount of 5% aqueous sodium citrate with initial molar ratio of citrate to Au^{3+} was added. The reaction was allowed to run until the solution reached a wine red color, indicating the reaction was completed.

Au nanoparticles	Surface composition	FL intensity (a.u.)
BSA-Au nanoclusters	BSA: 583 Amino acid residues Lots of carboxyl and amino groups	9978 (650 nm)
Tys-Au nanoclusers	Tys: 229 Amino acid residues some carboxyl and amino groups	1827 (703 nm)
GSH-Au nanoclusters	GSH: 3 Amino acid residues A little carboxyl and amino groups	966 (618 nm)
Citrate-Au nanoparticles	Citrate: carboxyl groups	No fluorescence

Table 1S Different active sites and FL intensity of different Au nanoparticles

3. Characterizations

Transmission electron microscopy (TEM) images and high-resolution TEM images were performed on JEM-2010 microscope (JEOL Co., Japan) at 200kV. Dynamic light scattering (DLS) and Zeta potential were recorded in Zeta sizer Nano ZS (Malvern Co., UK). XPS measurements were carried out on an ESCA Lab 250Xi (Thermo Scientific, USA). The Fourier Transform Infrared (FT-IR) spectrum was obtained from IS10 Fourier transform infrared (FT-IR) spectrophotometer (Thermo Inc., America). The CD spectrum was recorded using the Circular dichroism instrument. All fluorescence and CL spectra were performed on a fluorescence spectrophotometer (F-7000, Hitachi Co, Japan) with instrument settings: 700 V of high voltage, 10 nm excitation and emission slit. The UV-Vis absorbance spectra were obtained with a U-2910 UV-Vis spectrometer. The electron spin resonance (EPR) spectra were recorded with Bruker E-500. THF derivatives were also analyzed by HPLC on waters ACQUITY UPLC M-Class with a Zorbax SB-C18 reverse phase column (4.6×150mm, 5 μm) and an isocratic eluent (10% methanol and 90% water) at a flow rate of 1.0 mL/min. The GC - MS was used by GCMS-QP2010 Plus (SHIMADZU, Japan) to analyze the mixture after the reaction. The CL experiments were detected by the Ultra Weak Luminescence Analyzer (BPCL-2-TGC, Beijing) under ambient conditions with 0.1 s interval at 875 V.

4. Chemiluminescent tests

The CL light was detected by the static injection CL analysis with a 2 mL CL quartz vial adjacent to the photomultiplier

tube (PMT). Typically, 100 μl THF containing THF-HPO was placed in the quartz vial, then 900 μl BSA - Au NCs - Cu^{2+} mixture was quickly injected by a flow pump (BT100-02). When injected into the quartz vial, the reaction was initiated, the CL signals were recorded by PMT and the peak height was as deemed to the CL intensity.

5. Quantifying peroxides by iodometry

Typical procedure is as follows; A solution of dry THF (5 mL) in a Pyrex test tube was bubbled with O_2 and irradiated externally with 400 W high pressure mercury lamp for 20 h.[5] The product was mixed with saturated aq. KI (1 mL), AcOH (6 mL) and $CHCl_3$ (3 mL), and store in dark conditions for 15 min. The result solution was titrated by 0.1 M aq. $Na_2S_2O_3$, and the volumes of aq. $Na_2S_2O_3$ required corresponded to the certain amount of peroxides after subtracting the volume of aq. $Na_2S_2O_3$ consumed for blank experiment.

6. The preparation of ROS

we prepared 10 mM solution of various ROS ($^1O_2$, O_2•⁻, ROO•, NaClO, RO•, and •OH) by adding reagents as follows:: superoxide solution ($O_2^{-}\cdot$) was prepared by adding KO_2 (7 mg) to dry dimethyl sulfoxide (10 mL) and stirred vigorously for 10 min; singlet oxygen ($^1O_2$) was chemically generated by the reaction between H_2O_2 (10 mM) and NaClO (10 mM); H_2O_2: 30% H_2O_2 solution diluted to 10 mM, HOCl: 10 mM NaOCl, alkoxyl radical (RO·) was generated as a product of t-BuOOH (100 mM) in the presence of Fe(II) (10 mM); ROO• was generated as a product of CH3COOOH(100 mM) in the presence of Fe(II) (10 mM)and hydroxyl radical (·OH) was generated from the reaction of Fe(II) (1 mM) with H_2O_2 (10 mM).

Results and discussion

1. Characterization analysis of BSA-Au NCs

The successfully prepared Au NCs was displayed in TEM image and the hydrodynamic diameters was about 3 nm in the insert of Figure S1A. The UV-Vis spectrum of BSA capped gold clusters had a similar strong absorption to BSA at about 278 nm. As shown in Figure A1B, it has a continuous band on the higher energy side and no surface plasmon resonance was observed, which suggesting the size of particles were smaller than 2 nm. The fluorescence emission of Au NCs was around 650 nm upon excitation at different wavelength (Figure S1C). The prepared Au NCs was also analyzed by XPS. The Au 4f7/2 spectrum could be deconvoluted into two distinct components (red and blue curves) centered at binding energies of 84.1 and 85.1 eV, which could be assigned to Au (0) and Au(I), respectively (Figure S1D). Besides, The Fourier transform infrared (FTIR), far-UV circular dichroism (CD) analyses strongly suggested the formation of Au NCs. These data were consistent with the previously reported results.

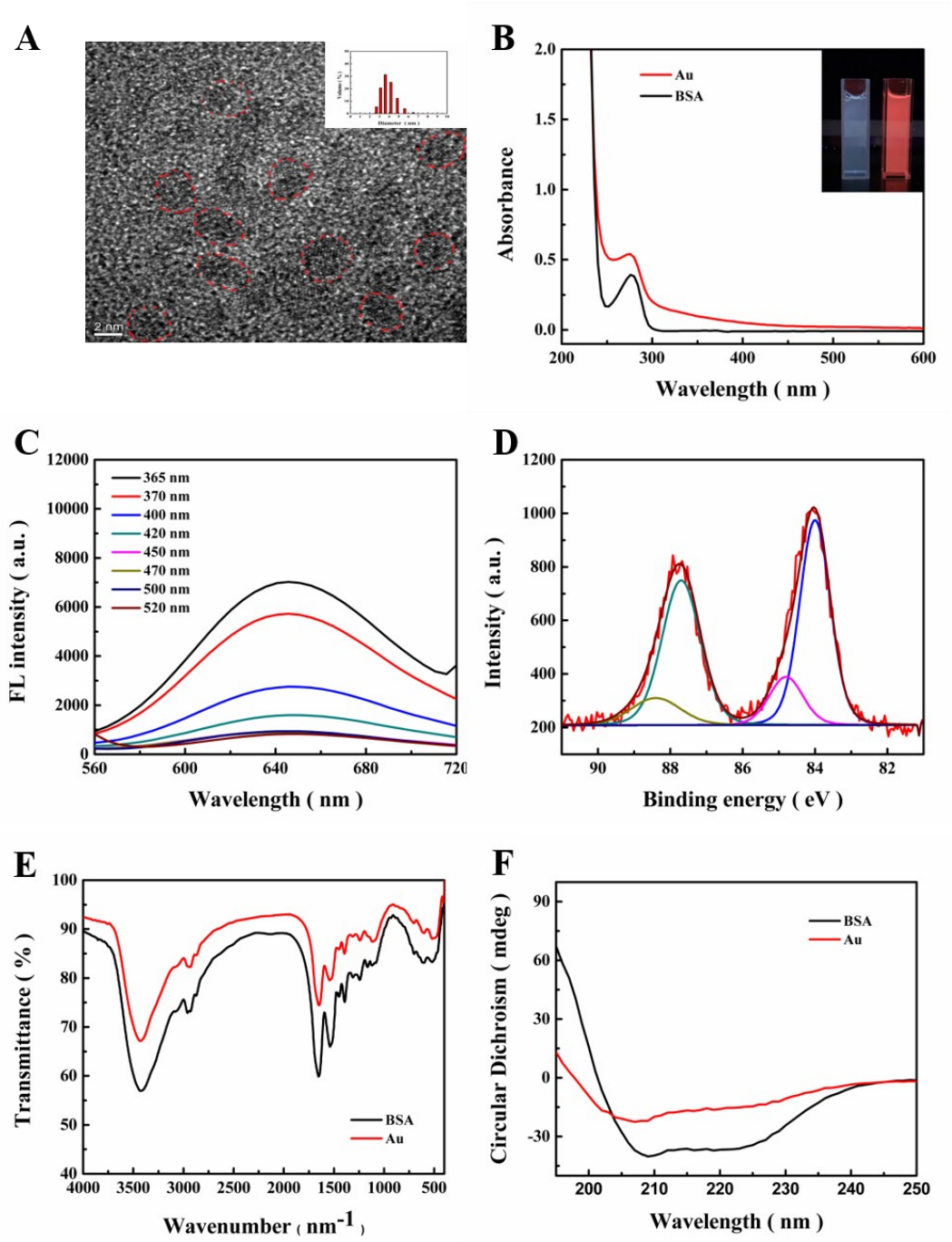

Figure S1. (A) Representative TEM images of BSA-Au NCs. The inset in (a) shows the DLS histograms. (B) Optical absorption spectra. The inset shows the photographs of Au NCs under visible and ultraviolet light (365 nm). (C) Photoemission spectra with different excitation., (D) XPS spectra of Au 4f for BSA Au NCs, and (E) Fourier-transform infrared (FTIR) spectra, (F) far-UV circular dichroism (CD) spectra of BSA (black) and BSA-Au NC bioconjugates (red).

2. The CL intensity in the influences of metal ions

The CL signals were obtained using the static injection CL analysis. Different kinds of metal ions were mixed with the BSA-Au NCs, then, the above mixture was added into the THF-HPO and the CL curve was detected. The data was shown in **Table S2**. A dozen times stronger CL signal was obtained when mixed with Cu^{2+}, and no same effect was

observed with the other metal ions.

Cu^{2+}	Fe^{2+}	Co^{2+}	Cr^{3+}	Cd^{2+}	Mn^{2+}	Sn^{4+}	Sn^{2+}	Pb^{2+}
21649	1949	1462	1909	3563	1792	2792	2185	909
Zn^{2+}	Ni^{2+}	Ce^{4+}	Bi^{3+}	Al^{3+}	Fe^{3+}	Na^{+}	Ca^{2+}	Ag^{+}
2243	1432	1897	1397	1534	1525	1348	1539	1252

Table S2. The effects of metal ions on the CL intensity.

3. Optimizing conditions

Considering to the effects of reactant conditions on the CL system, we optimized the order of injection, the flow rate of pump, pH, the nanoparticle diameter, concentration, etc. It was found that the system had a highest CL in acidic condition (pH=2), which might be due to the peroxide decomposed easily when faced strong acid and the solubility of copper ions (K_{SP} [$Cu(OH)_2$]$=2.2\times10^{-20}$).

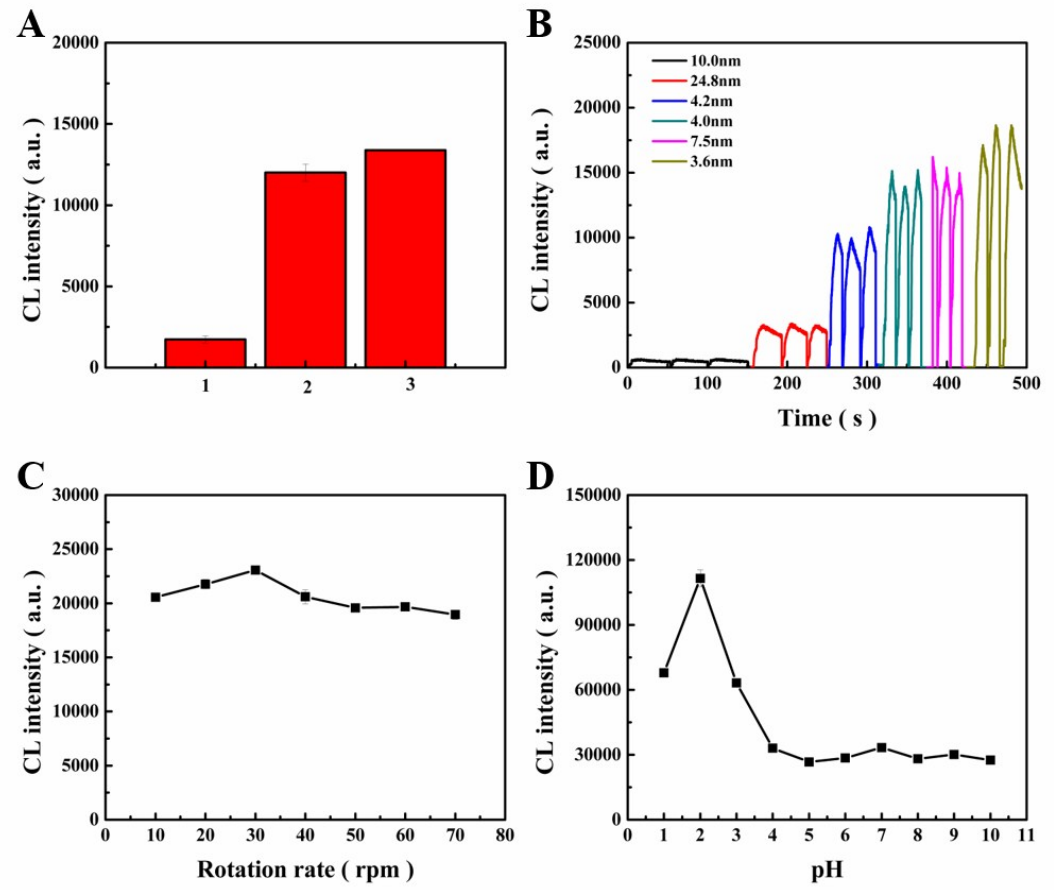

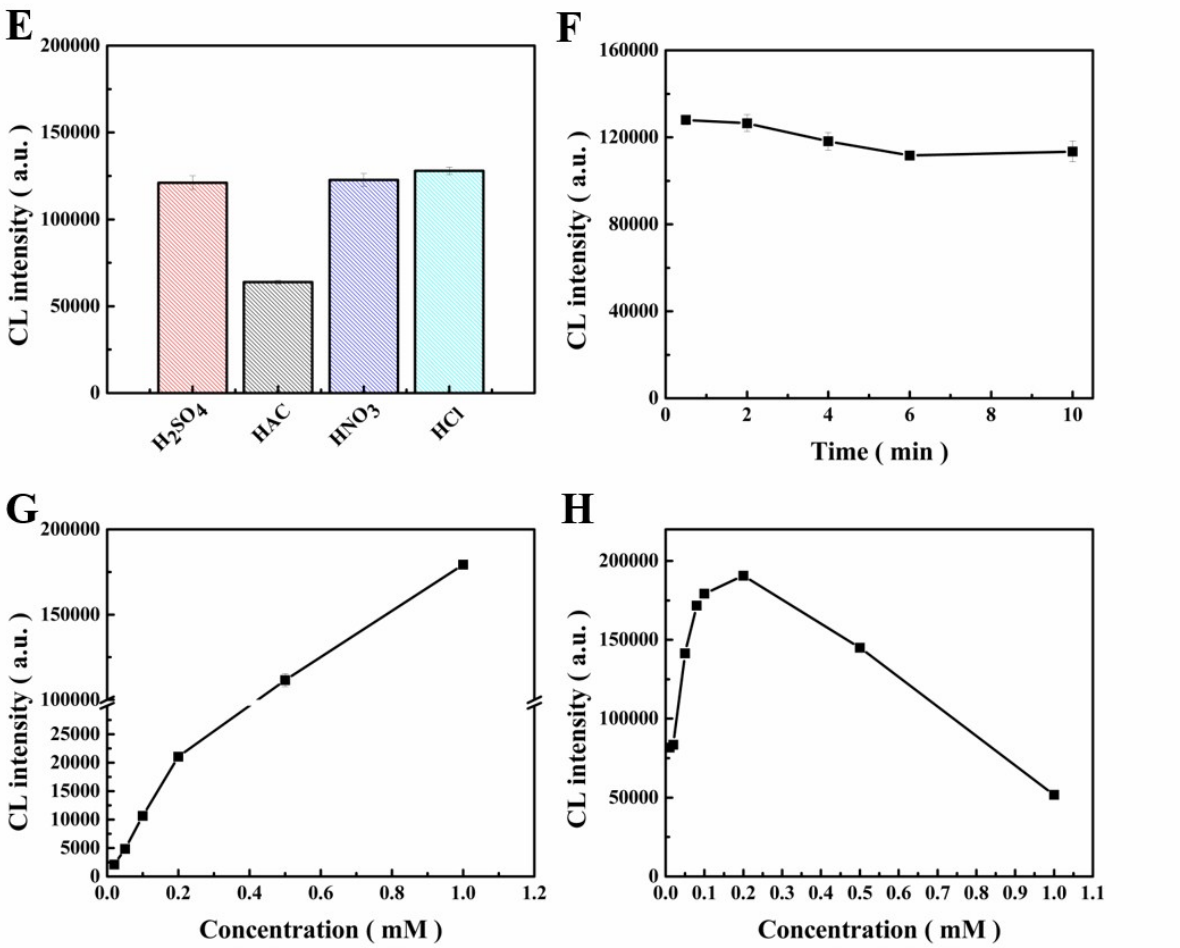

Figure S2. Effects of (A) the order of injection, (1) adding Cu^{2+} to the mixture of THF-HPO and BSA-Au NCs, (2) adding the mixture of THF-HPO and Cu^{2+} to BSA-Au NCs, (3) adding the mixture of Cu^{2+} and BSA-Au NCs to THF-HPO. (B) the nanoparticle diameter. (C) the rotation rate of pump. (D) pH. (E) different acids media on CL intensity. (F) the time of injection. Conditions: THF-HPO 3.5 mM, BSA-Au NCs 0.02 mM, Cu^{2+} 2.0×10^{-4} M. Influence of concentrations of (G) BSA-Au NCs and (H) Cu^{2+} solution the CL intensity.

4. The characteristics of BSA-Au NCs after reaction with THF-HPO

After CL reaction, we measured the properties of the BSA-Au NCs using optical spectrometer, DLS, Zeta potential and XPS spectrums. reaction. The transformation of BSA-Au NCs to the large size was confirmed by the DLS measurement. In the Au 4f spectrum of the BSA-Au NCs after reactions, the percentage of the binding energies at 84.1 eV assigned to Au (0) became less, and the binding energies at 85.1 eV assigned to Au(I) increased, respectively. This result was consistent with the DLS measurement.

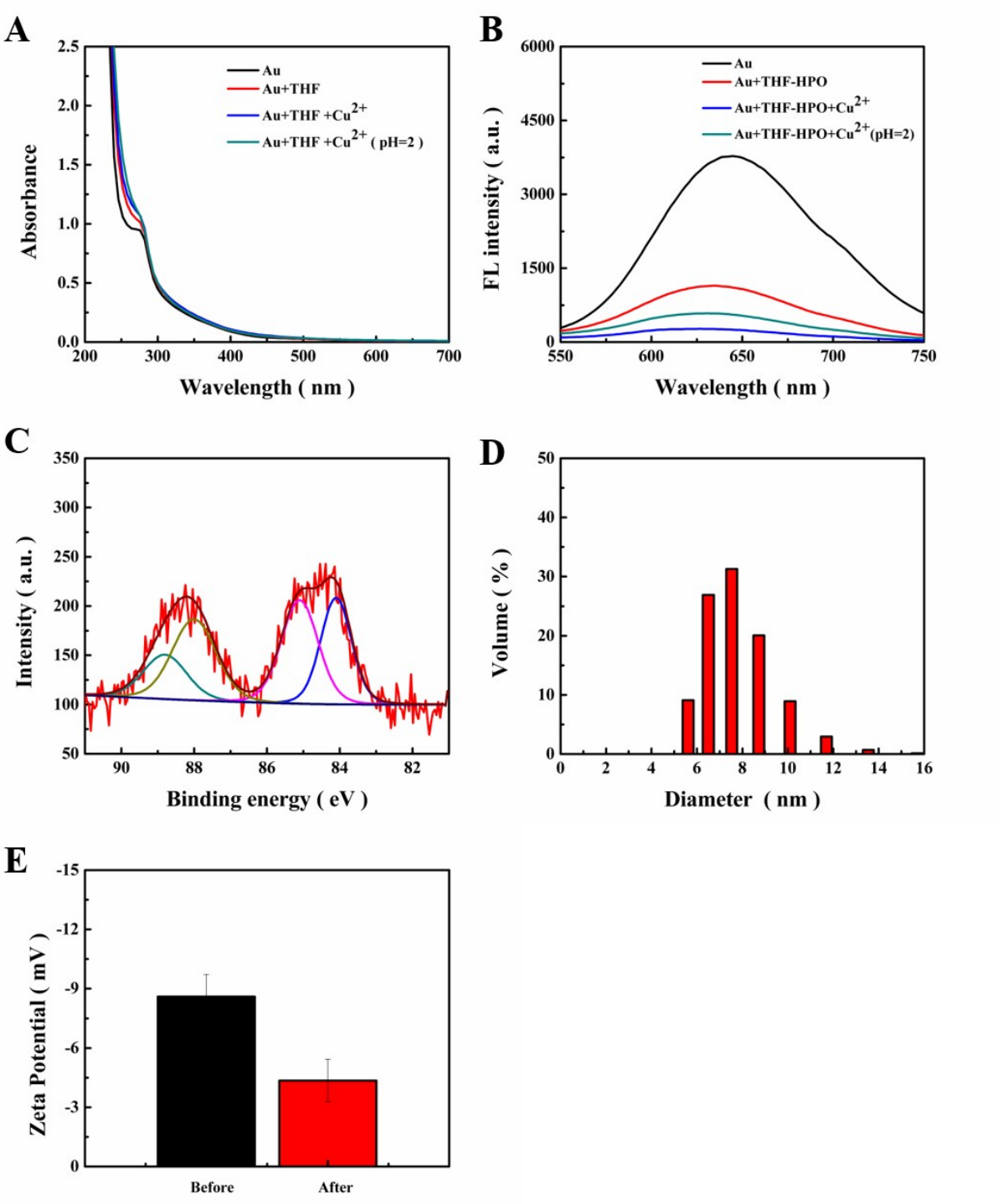

Figure S3. (A) Optical absorption spectra. (B) Photoemission spectra with excitation at 365 nm. (C) XPS spectra of Au 4f, (D) DLS histograms, and (E) Zeta potential for BSA Au NCs after the reaction with THF-HPO. Conditions: THF-HPO 5 mM, BSA-Au NCs 0.02mM, Cu^{2+} 2.0×10^{-4} M.

5. The effect of dissolved oxygen on the CL intensity

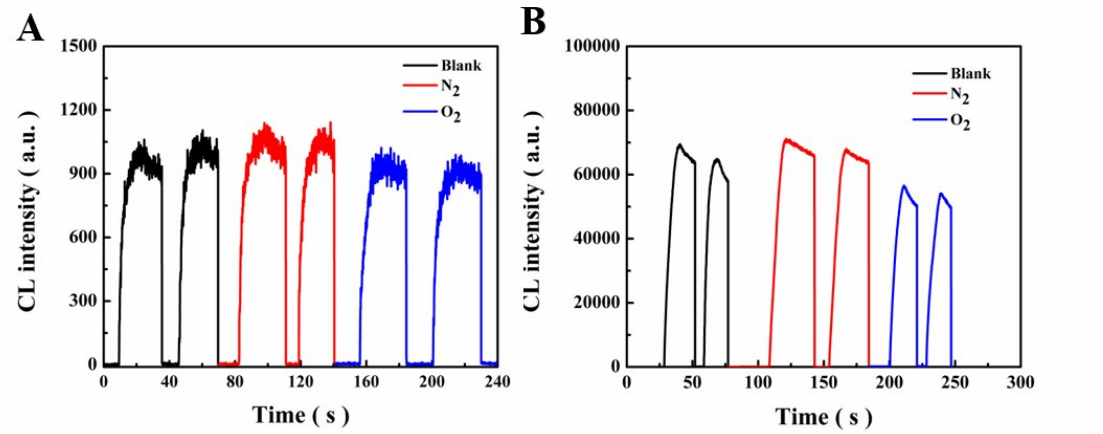

Figure S4. The kinetic curves of BSA-Au NCs-THF-HPO CL systems: (A) without metal ions, (B) Cu^{2+}, the CL solution was bubbled with N_2 (red) or O_2 (blue) for 30 min before injecting. Conditions: BSA-Au NCs 0.04mM, THF-HPO 0.3mM, Cu^{2+} 2.0×10^{-4} M.

6. The effects of different active oxygen radical scavengers on the CL emission.

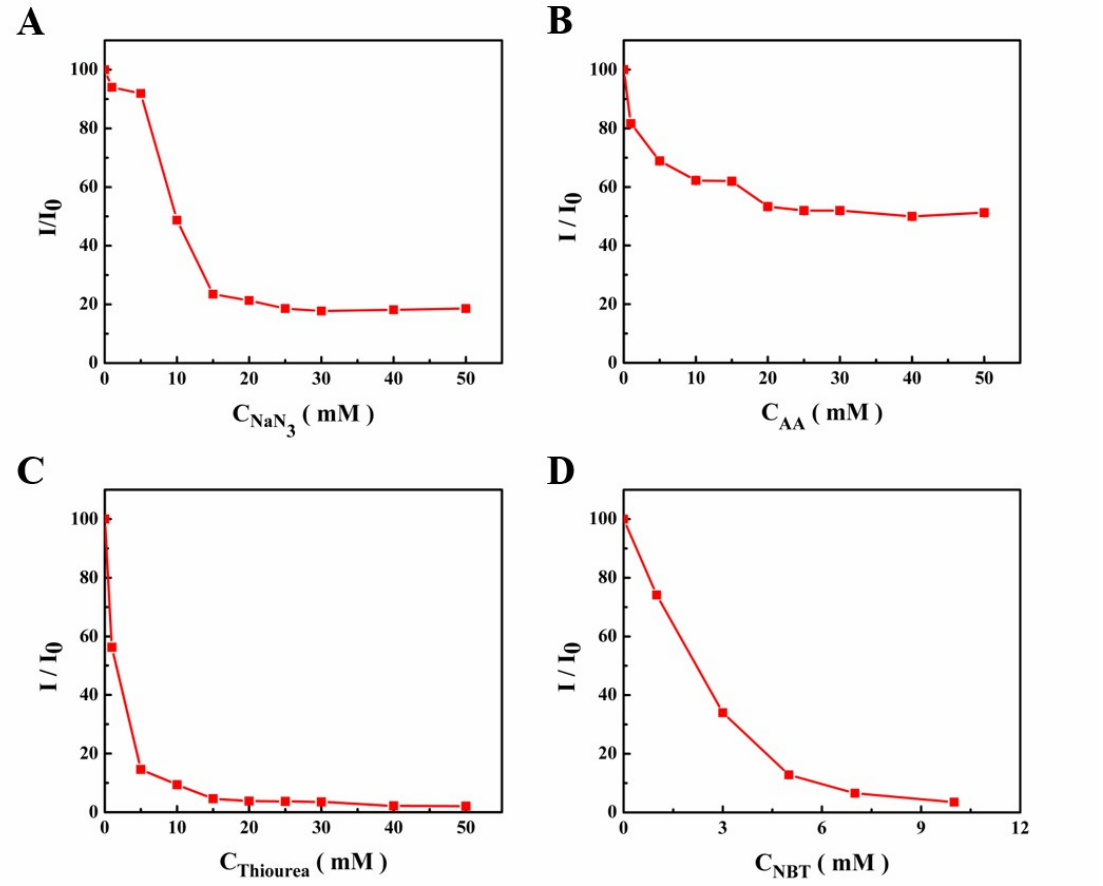

Figure S5. E□ects of the radical scavengers of (A) Na3N, (B) AA, (C) thiourea, and (D) NBT on the BSA-Au NCs-Cu^{2+}-THF-HPO CL system. Final concentrations: THF-HPO 0.5 mM, BSA-Au NCs 0.02 mM, Cu^{2+} 2.0×10^{-4} M.

7. The study of probable mechanism of the CL system.

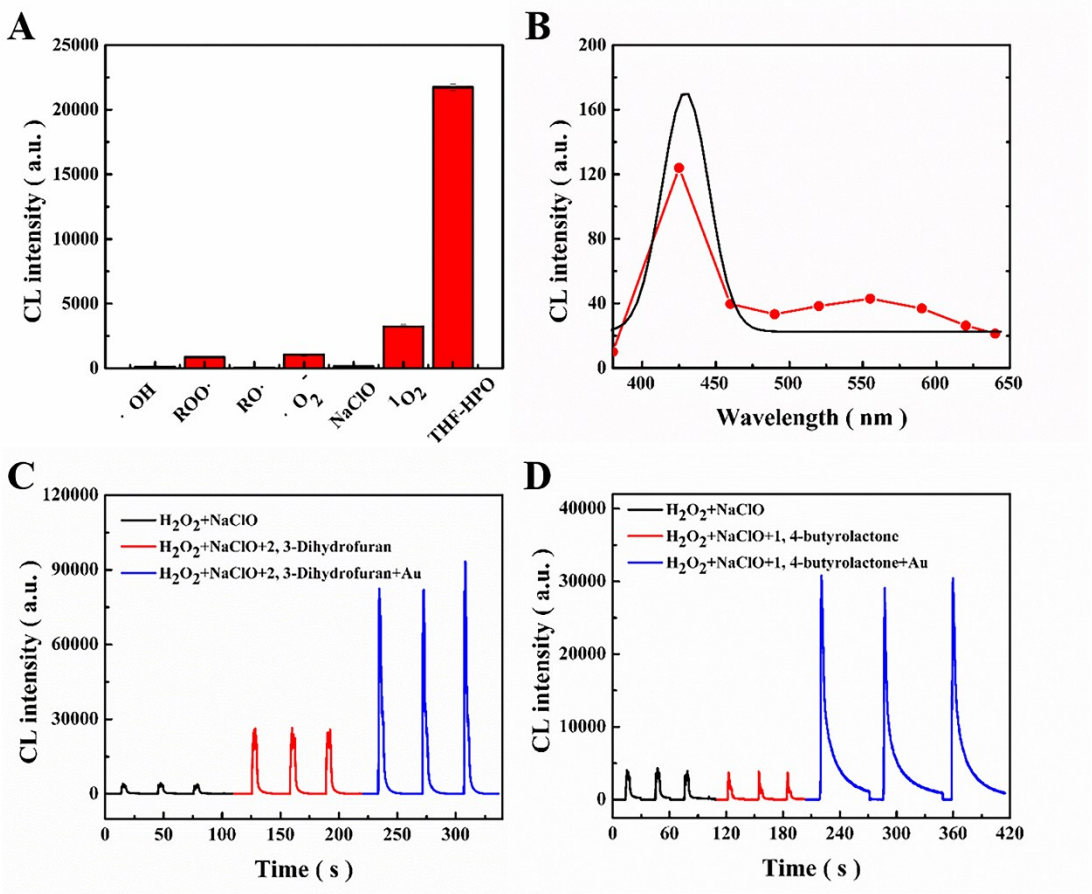

Figure S6. (A) The CL intensity of Au@BSA NCs towards different kinds of ROS. (B) CL spectra of the THF-HPO- $\bullet O_2^-$ systems. The CL curve of (C) the 2,3-dihydrofuran-$^1O_2$-Au@BSA NCs and (D) 1,4-butyrolactone-$^1O_2$-Au@BSA NCs systems. Conditions: H_2O_2 and NaClO 10 mM, (C) Au@BSA NCs 0.4 mM, and (D) Au@BSA NCs 4 mM.

8. Hydroxyl and superoxide anion radicals in several peroxides.

As described in the scavenger tests, it indicated that the $\bullet O_2^-$ anionic radical and •OH had a strong relationship with CL emission. Meanwhile, it is well-known that $\bullet O_2^-$ anionic radical and •OH are involved in electron–hole annihilation which induced CL amplification. These radicals in the control tests which use other peroxides instead of THF-HPO were measured by spectrophotometry. The determination of •OH and $\bullet O_2^-$ anionic radical relied on the change of absorption of methylene blue and NBT, respectively. For the determination of •OH generated from the tests: the solution containing methylene blue mixed with peroxides was detected the absorption at about 620 nm, then 0.3 mM gold nanoclusters was added into the above solution at the same concentration, gold nanoclusters could induce peroxides decompose into radicals and methylene blue could reacted with •OH to form hydroxylated methylene blue, the changes of the absorption was recorded as the amount of hydroxyl radicals. In the same way, NBT could react with $\bullet O_2^-$ to produce formazan and the absorption at about 520 nm could change when the solution with or without BSA-Au NCs, indicating the amount of $\bullet O_2^-$ in the systems.

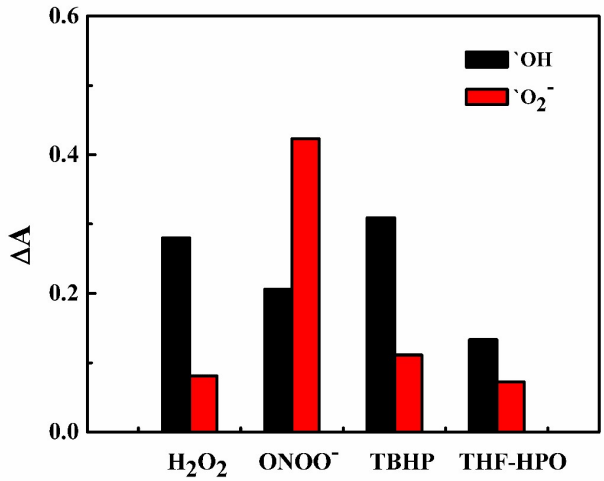

Figure S7. Changes of the absorption of the different peroxide solution containing methylene blue and NBT in the presence/absence of BSA-Au NCs. (Black column: •OH, red column: $•O_2^-$). Conditions: BSA-Au NCs 0.02mM, peroxides 1mM, methylene blue 0.01mg/ml, NBT: 1mM.

9. General oxidant selectivity study.

In the static injection CL system for selectivity study, different oxidant was placed in the quartz vial, then the mixture of Cu^{2+} and BSA-Au NCs solution was injected, followed by the collection of CL signal. The response of inorganic oxidants to the mixture solution was about several hundreds, this CL phenomenon might be attributed to the oxidation reaction of BSA. As shown in Figure S8B, it was same as the above results, the slightly obvious CL intensity when injected into $ONOO^-$ was also because of the decomposition easily in acidic conditions and the existence of BSA.

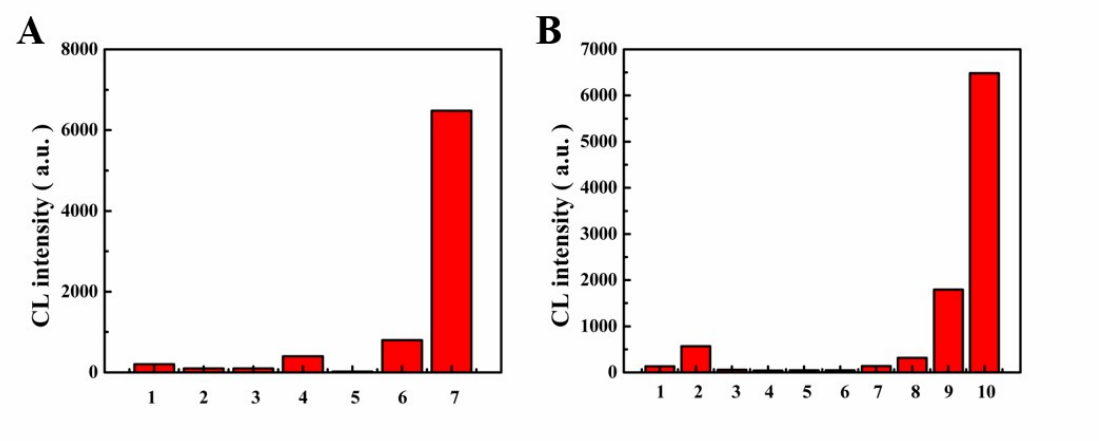

Figure S8. Luminescence intensity of BSA-Au NCs in the presence of different commonly used

(A) inorganic oxidants: (1) $K_3[Fe(CN)_6]$, (2) $K_2S_2O_8$, (3) $KMnO_4$, (4) KIO_4, (5) $K_2Cr_2O_7$, (6) Ce^{4+}, (7) THF-HPO, and (B) peroxides: (1) H_2O_2, (2) H_2O_2+$NaHCO_3$, (3) TBHP, (4) TBPB, (5) BPO, (6) CH_3COOOH, (7) MEKP, (8) H_2O_2+Na_2SO_3, (9) $ONOO^-$, (10) THF-HPO. Conditions: BSA-Au NCs 0.02 mM, Cu^{2+} 2.0×10^{-4} M, pH=2, THF-HPO 0.5mM, other oxidants1mM.

10. Oxidation of tryptophan in BSA-Au NCs by peroxides.

The tryptophan could be oxidized by the peroxides to produce any tryptophan metabolites, which could emit at 558 nm. The amount of oxidized tryptophan was detected by synchronous fluorescence analysis：Setting the voltage of photomultiplier tube of fluorescence spectrophotometer at 700eV, the slit width of excitation and emission are both 10 nm, △λ=60 nm, then the fluorescence of BSA-Au NCs solution before and after added peroxides was measured, the fluorescence intensity at about 280 nm was considered as the amount of tryptophan.

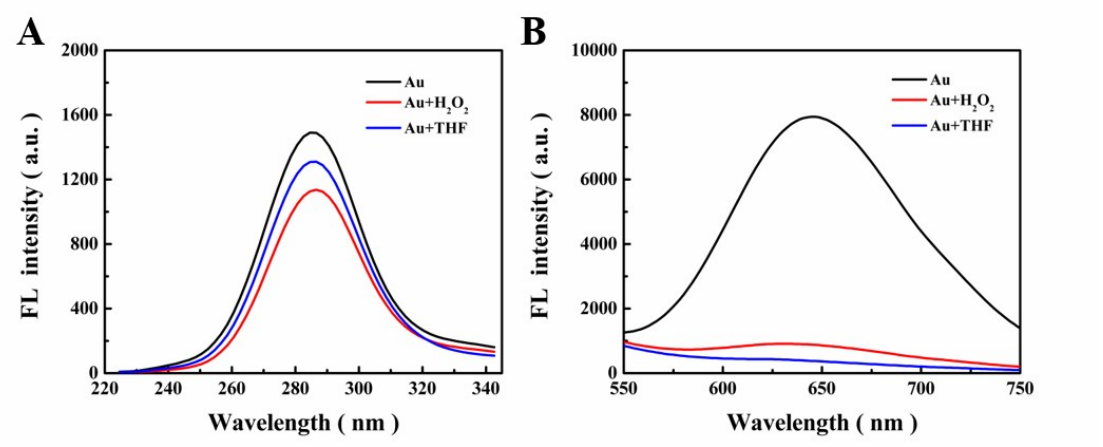

Figure S9. The fluorescence spectra of (A) tryptophan and (B) BSA-Au NCs in BSA-Au NCs solution in the absence/presence of different peroxides. Conditions: BSA-Au NCs 0.02 mM, Cu^{2+} 2.0×10^{-4} M, THF-HPO 10mM, H_2O_2 10mM.

11. CL intensity of the reaction of other ether peroxides and BSA-Au NCs.

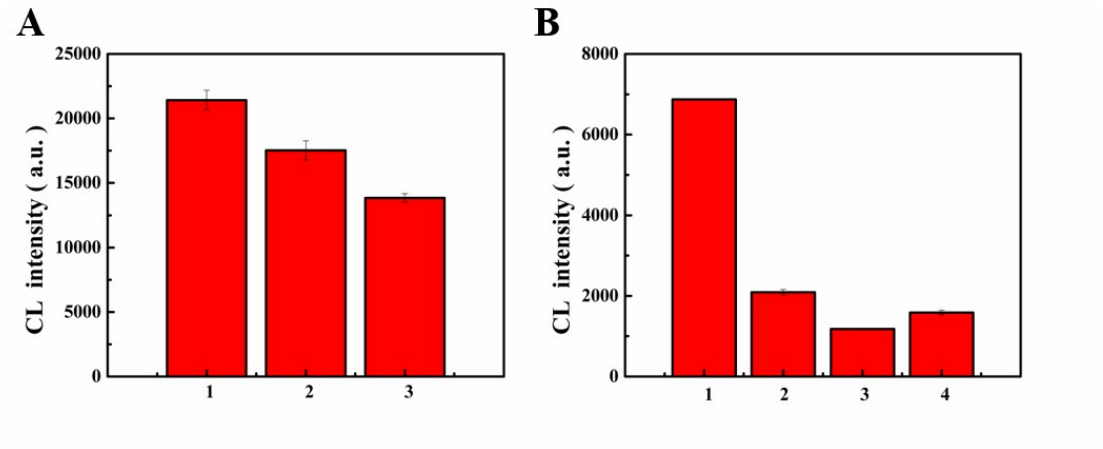

Figure S10. The CL intensity of BSA-Au NCs in the presence of different ether peroxides. Conditions: BSA-Au NCs 0.02mM, THF-HPO 10mM, Ethylene glycol ether peroxide 7.2mM, Ethylene glycol methyl ether peroxide 7.4mM, Ethylene glycol dimethyl ether peroxide 4mM, Diethylene glycol monoethyl ether peroxide 3mM, 1-Methoxy-2-propanol peroxide 2mM, 2-(2-Methoxyethoxy) ethanol peroxide 2mM.

12. The characteristics of THF-HPO before and after the reaction with BSA-Au NCs.

HPLC and FTIR were applied to study the feature of the THF-HPO before and after reactions. It was obvious that only

one peak with retention time at about 4.45 min, which meant the THF solution just contained THF-HPO. This result was consistent with the FTIR spectrum. It should be noted that the small absorption peak from 1600-1800 cm^{-1} might be attributed to the CO_2 dissolved in solution, which was also detected in ethanol. After the CL reaction, the obvious absorption peak at about 1780 cm^{-1} assigned to C=O was shown in FTIR. It indicated the organic product was an organic molecule having carbonyl groups. The similar phenomenon was verified by the GC-MS. At the retention time of 2.315 min and 12.563 min, there was a peak belongs to 2,3-Dihydrofuran and 1,4-butyrolactone, respectively.

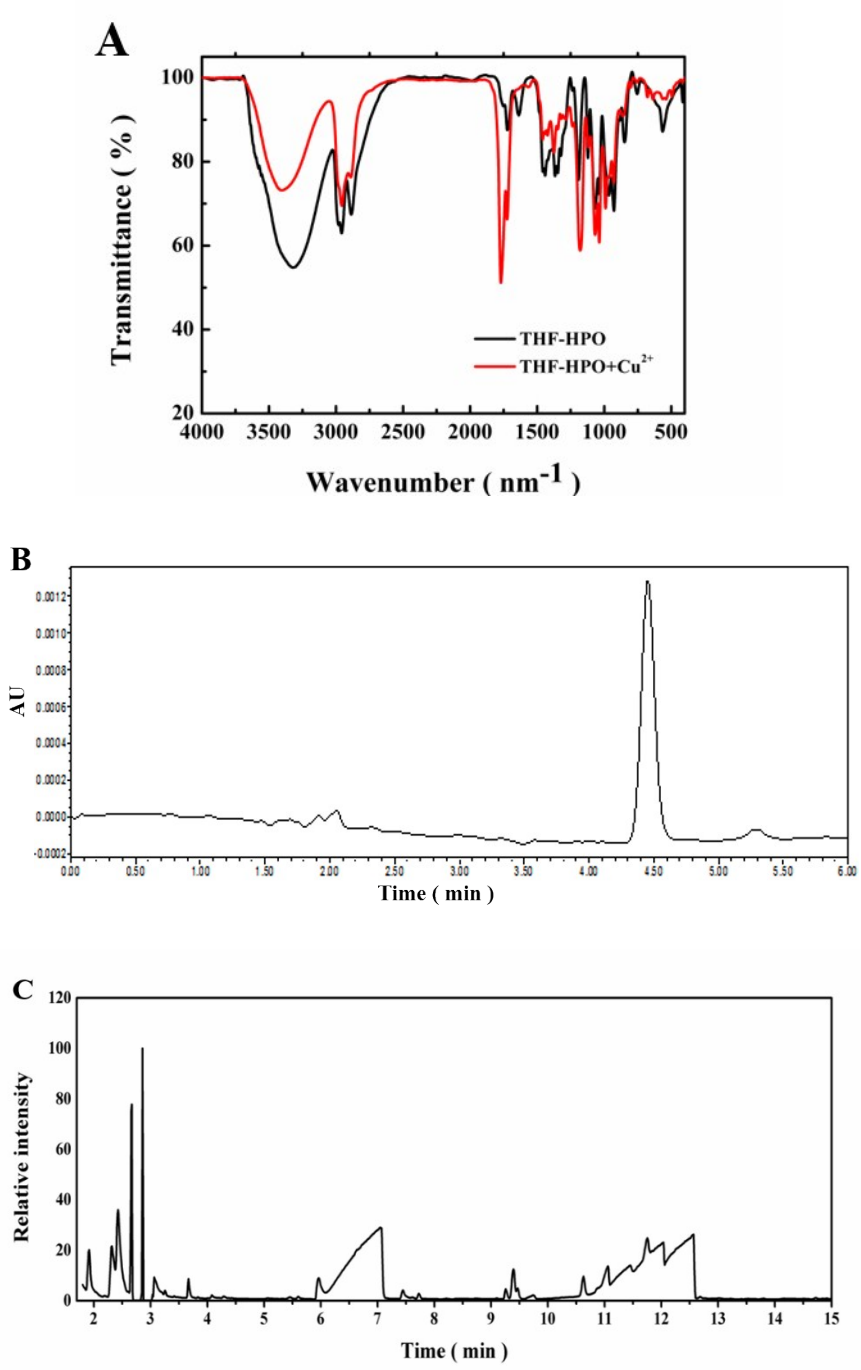

Figure S11. (A) FTIR spectra of THF-HPO before and after the reaction with Cu^{2+}. (B) HPLC analysis of THF-HPO. (C) GC-MS analysis of THF-HPO after reaction of the CL system.

13. Schematic illustration of CL mechanism in the BSA-Au NCs-THF-HPO-Cu^{2+} system.

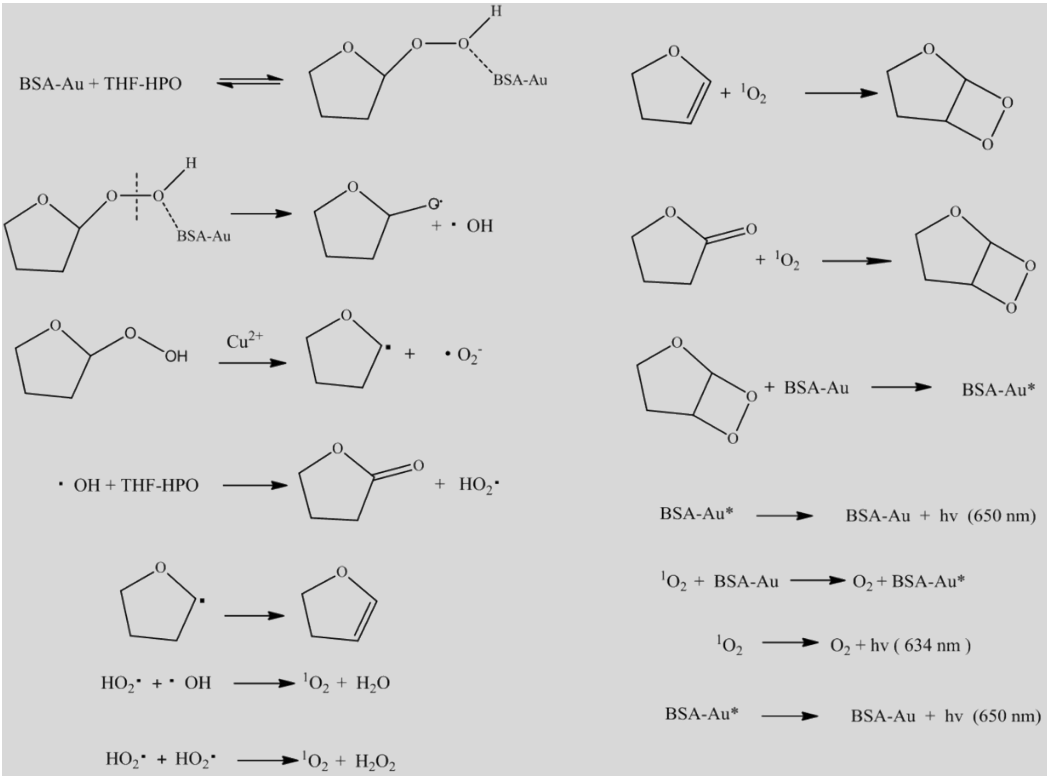

Figure S12. Proposed CL mechanism of the BSA-Au NCs-THF-HPO-Cu^{2+} system.

14.The application of the CL system for detection of ether peroxides and Cu^{2+}.

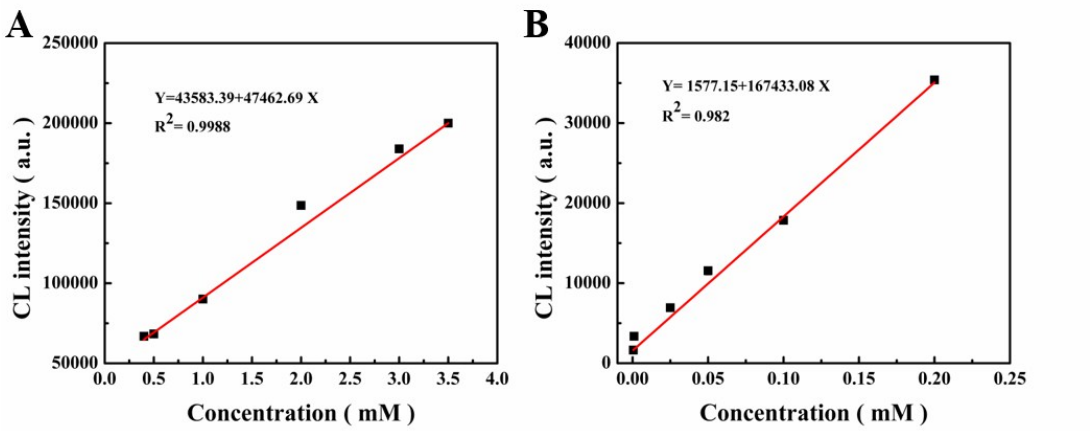

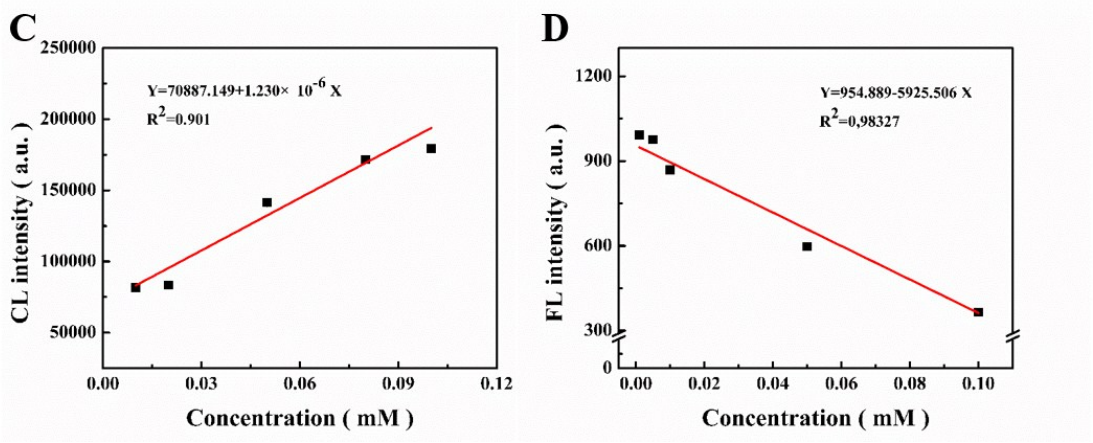

Figure S13. (A) and (B) Linear relationship between CL intensities with different concentration THF-HPO, (C) and (D) Linear relationship between CL/FL intensities with different concentration Cu^{2+}, respectively. Conditions: (A) and (B): BSA-Au NCs 0.04 mM, Cu^{2+} 2.0×10^{-4} M, (C) and (D) BSA-Au NCs: 0.04 mM, THF-HPO 10mM.

References:

1. J. Xie, Y. Zheng and J. Y. Ying, *Journal of the American Chemical Society*, 2009, **131**, 888-889.
2. Y. Xu, J. Sherwood, Y. Qin, D. Crowley, M. Bonizzoni and Y. Bao, *Nanoscale*, 2014, **6**, 1515-1524.
3. Y. Xie, Y. Xianyu, N. Wang, Z. Yan, Y. Liu, K. Zhu, N. S. Hatzakis and X. Jiang, *Adv. Funct. Mater.*, 2018, **28**, 1702026.
4. Z.-F. Zhang, H. Cui, C.-Z. Lai and L.-J. Liu, *Analytical Chemistry*, 2005, **77**, 3324-3329.
5. N. Tada, T. Ishigami, L. Cui, K. Ban, T. Miura and A. Itoh, *Tetrahedron Lett.*, 2013, **54**, 256-258